Tanks in Series Model for Continuous Stirred Tank Electrochemical Reactor

R. Saravanathamizhan, R. Paranthaman, and N. Balasubramanian*

Department of Chemical Engineering, A.C. Tech Campus, Anna University-Chennai, Chennai-600025, India

C. Ahmed Basha

Department of Pollution Control, Central Electrochemical Research Institute, Karaikudi-630 006, India

It is attempted in the present investigation to study the residence time distribution of electrolyte in a continuous stirred tank electrochemical reactor. The electrolyte flow behavior has been experimented on by using both pulse and step input techniques. The exit age distribution curves obtained under various operating conditions are critically analyzed. A theoretical model based on *tanks in series* has been developed to describe the electrolyte flow behavior inside the continuous stirred tank electrochemical reactor, and the model simulations are validated with experimental observations.

Introduction

Day-to-day human activities and the industrial revolution have influenced the generation of large quantity of effluent. The treatment of industrial effluent has become indispensable as such effluent contaminates bodies of water and may be toxic to many life forms. Since most of the industrial effluents are difficult to degrade, the disposal of industrial effluent has become a major environmental issue. In general, industrial effluents are characterized to have a large amount of suspended solids, high chemical oxygen demand and biological oxygen demand, and varying pH.

Conventionally, industrial effluents are treated by physical, chemical, and biochemical techniques. Because of the large complexity of the composition of effluent, most of these traditional methods are becoming inadequate. As the environmental regulations becoming more stringent day by day, new and novel processes for efficient treatment of effluent at low operating cost are needed. In this perspective, researchers are focusing on advanced oxidation processes such as electrochemical technique, wet air oxidation, ozonation, and a photocatalytic method for the degradation of organic compounds present in the wastewater. Among these advanced oxidation processes, electrochemical treatment has been receiving greater attention due to its unique features such as complete degradation without generation of solid sludge, energy efficiency, automation, and cost effectiveness.[1,2]

In electrochemical technique, electron is used to degrade all the organics present in the effluent without generating any secondary pollutant or biproduct/sludge. The advantage of the electrochemical technique is high removal efficiencies with low temperature requirements compared to nonelectrochemical treatment. In addition to the operating parameters, the pollutant degradation rate depends on the anode material. When electrochemical reactors operate at high cell potential, the anodic process occurs in the potential region of water discharge and hydroxyl radicals are generated. On the other hand, if chloride is present in the electrolyte, an indirect oxidation via active chlorine can be operative,[3] which has been successfully adopted for treatment of several industrial effluents. In our earlier investigations, in situ catalytic oxidation of textile effluent using oxide coated electrodes and the reuse of treated wastewater for dyeing applications have been attempted.[4−6]

Different types of electrochemical reactors ranging from conventional plate and frame cell to advanced electrodes such as three-dimensional electrodes are used for electrochemical processes. The design or selection of suitable electrochemical reactor is very important in electrochemical process as the reactor geometry plays an important role in the process yield.

Extensive work has been reported on the analysis of performance of various electrochemical reactors. Bengoa et al.[7] studied the flow behavior of electrolyte in a filter press type electrochemical reactor and reported residence time distribution using a commercial ElectroSyn cell. The authors observed both the axial and lateral dispersion phenomena in a plug flow behavior. Lidia and Marta[8] have experimented the treatment of textile effluent of reactive dye Red Procion H-EXGL using an electrochemically generated redox mediator in a filter press cell and developed a model for exit age distribution. The authors reported that the electrolyte flow behavior is close to plug flow. Trinidad and Walsh[9] verified dispersion and Schneider−Smith models for a laboratory filter press reactor using the pulse tracer technique and observed wide deviation of these models from the ideal plug flow model, while the authors[10] reported the conversion expression for batch, plug flow, and continuous stirred electrochemical reactors in terms of mass transfer coefficient.

Carpenter and Roberts[11] studied the mass transport and residence time distribution in a parallel-plate flow oscillatory electrochemical reactor for the reduction of ferricyanide and reported that the oscillatory flow enhances the mass transport rate. Jose Gonza lez-Garcya et al.[12] studied the hydrodynamic behavior in a filter-press electrochemical reactor, assembled with three-dimensional carbon felt electrodes. Polcaro et al.[13] experimented water disinfection process and hydrodynamics study in a stirred tank electrochemical reactor using a boron-doped diamond electrode and developed model for two CSTERs in parallel configuration.

The flow characteristic of electrolyte in an electrochemical reactor is of great importance. The objective of the present investigation is to study the residence time distribution in a continuous stirrer tank electrochemical reactor. A theoretical model based on “tanks in series” has been proposed to describe the electrolyte flow behavior, and the model simulations have been verified with the experimental observations.

---

* Corresponding author. E-mail: nbsbala@annauniv.edu. Tel.: 91-44-22203501.

10.1021/ie071426q CCC: $40.75

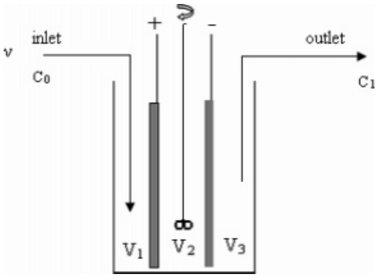

Figure 1. Schematic of the continuous stirred tank electrochemical reactor.

Continuous Stirred Tank Reactor Model

Let us consider a simple electrode reaction as given below

$$A + ne^- \leftrightarrow B^+ \tag{1}$$

where "n" refers to number of electrons. The above reaction can be controlled by either by kinetic or mass transfer. The limiting current density can be related to the mass transfer coefficient as[14]

$$i_L = nFk_mC \tag{2}$$

where k_m refers to the mass transfer coefficient and C refers to the bulk concentration. If the reaction takes place in a continuous stirred tank electrochemical reactor [Figure 1], then the material balance can be written as

$$v(C_{Ai} - C_A) = \frac{iS}{nF} \tag{3}$$

The eq 3 can be written in term of residence time as

$$C_{Ai} - C_A = \frac{\sigma\tau i}{nF} \tag{4}$$

where C_{Ai} and C_A refer to initial and final concentrations and σ refers to the interfacial area of the electrode. The electrode kinetics is assumed to follow Butler−Volmer type equation, i.e.

$$\frac{i}{nF} = k_1C_A^S - k_2C_B^S \tag{5}$$

where k_1 and k_2 represent the reaction rate constants for forward and reverse reactions, respectively, and C_A^S and C_B^S are surface concentrations. The current density can be expressed in terms of the mass transport of A for steady-state operation as

$$\frac{i}{nF} = k_{L1}(C_A - C_A^S) \tag{6}$$

where k_{L1} represents the mass transfer coefficient of A. The eq 6 can be written in terms of mass transport of B as

$$\frac{i}{nF} = k_{L2}(C_B^S - C_B) \tag{7}$$

where k_{L2} represents the mass transfer coefficient of B. Combining eqs 5−7, the surface concentration is eliminated resulting the reaction rate in terms of bulk concentration,[15] i.e.

$$\frac{i}{nF} = \frac{k_1C_A - k_2C_B}{1 + \dfrac{k_1}{k_{L1}} + \dfrac{k_2}{k_{L2}}} \tag{8}$$

Substituting eq 8 in eq 5 and rearranging the equation results in

$$C_{Ai} - C_A = \sigma\tau\frac{k_1C_A - k_2C_B}{(1 + D_1 + D_2)} \tag{9}$$

where D_1 and D_2 are Damkohler numbers for the forward and reverse reactions, which can be defined as

$$D_1 = \frac{k_1}{k_{L1}} \quad \text{and} \quad D_2 = \frac{k_2}{k_{L2}}$$

The overall material balance for the reactor in terms of concentration can be written as

$$C_{Ai} = C_A + C_B \tag{10}$$

Substituting for C_B in eq 9 and rearranging the results gives

$$\frac{C_A}{C_{Ai}} = \frac{1 + \dfrac{\sigma\tau k_2}{(1 + D_1 + D_2)}}{1 + \dfrac{\sigma\tau(k_1 + k_2)}{(1 + D_1 + D_2)}} \tag{11}$$

For an irreversible reaction the term k_2 becomes zero, and then the eq 11 is reduced to

$$\frac{C_A}{C_{Ai}} = \frac{1}{(1 + P)} \tag{12}$$

where

$$P = \frac{\sigma\tau k_1}{(1 + D_1)}$$

The eq 12 represents the conversion equation for a continuous stirred tank electrochemical reactor. For CSTERs connected in series the eq 12 can be modified as

$$\frac{C_{AN}}{C_{AN-1}} = \frac{1}{1 + \dfrac{\sigma\tau k_1}{(1 + D_1)}} \tag{13}$$

where "N" represents the number of tanks in series. The eq 13 can be rearranged as[16]

$$\frac{C_{AN}}{C_{Ai}} = \left(1 + \frac{\sigma\tau k_1}{(1 + D_1)}\right)^{-N} \tag{14}$$

Tanks in Series Model

Tanks in Series model has been proposed to describe the flow characteristics of the electrolyte in a CSTER. It is assumed that the CSTER consists of three tanks connected in series [Figure 1]. Accordingly the tracer material balance for the tank 1 can be written as

$$\tau_1\frac{dC_1}{dt} = C_o - C_1 \tag{15}$$

where τ_1 represents the residence time of electrolyte in tank 1; C_o and C_1 refer to the inlet and outlet tracer concentration of tank 1. Similarly the tracer material balance can be developed for second and third tanks as given below.

The material balance for tank 2 can be written as

$$\tau_2 \frac{dC_2}{dt} = C_1 - C_2 \qquad (16)$$

The material balance for tank 3 can be given as

$$\tau_3 \frac{dC_3}{dt} = C_2 - C_3 \qquad (17)$$

where C_2 and C_3 represent tracer outlet concentrations of second and third tanks, respectively, while τ_2 and τ_3 represent the residence time of electrolyte in tanks 2 and 3, respectively. The model is further extended for age distribution analysis for the following conditions.

Case I: The volumes of the three tanks are unequal (i.e., $V_1 \neq V_2 \neq V_3$).

Case II: The volumes of the three tanks are equal (i.e., $V_1 = V_2 = V_3$).

Case III: The volumes of tanks 1 and 3 are equal, and the volume of tank 2 is higher than those of the other tanks (i.e., $V_1 = V_3$; $V_2 > V_1, V_3$).

All the above three cases have been considered for the simulation to find the active volume involved during the process in CSTER.

Case I: As stated earlier, it is assumed that the reactor has three tanks of unequal volume separated by the electrodes. The electrolyte enters at tank 1 and leaves at tank 3. The total volume of the reactor is the summation of the volumes of all three tanks, i.e.

$$V = V_1 + V_2 + V_3 \qquad (18)$$

where V_1, V_2, and V_3 represent the volumes of tanks 1, 2, and 3, respectively, and "V" refers to the reactor total volume. The exit age distribution analysis has been performed by both step and pulse input techniques. Solving the eqs 15 to 17 for the pulse input, the $F(t)$ can be written for the three tanks connected in series as (For all the three cases the analytical solution given in the annexure)

$$F(t) = \tau_1\left(\frac{\tau_1 e^{-t/\tau_1}}{(\tau_1 - \tau_2)(\tau_1 - \tau_3)} + \frac{\tau_2 e^{-t/\tau_2}}{(\tau_2 - \tau_1)(\tau_2 - \tau_3)} + \frac{\tau_3 e^{-t/\tau_3}}{(\tau_3 - \tau_2)(\tau_3 - \tau_1)}\right) \qquad (19)$$

Differentiating eq 19 results in the exit age distribution $E(t)$, i.e.

$$E(t) = \tau_1\left(\frac{e^{-t/\tau_1}}{(\tau_1 - \tau_2)(\tau_3 - \tau_1)} + \frac{e^{-t/\tau_2}}{(\tau_1 - \tau_2)(\tau_2 - \tau_3)} + \frac{e^{-t/\tau_3}}{(\tau_2 - \tau_3)(\tau_3 - \tau_1)}\right) \qquad (20)$$

Solving eqs 15−17 for the step input and rearranging results in the following expression for $F(t)$, i.e.

$$F(t) = 1 - \frac{{\tau_1}^2 e^{-t/\tau_1}}{(\tau_3 - \tau_1)(\tau_2 - \tau_1)} - \frac{{\tau_2}^2 e^{-t/\tau_2}}{(\tau_1 - \tau_2)(\tau_3 - \tau_2)} - \frac{{\tau_3}^2 e^{-t/\tau_3}}{(\tau_1 - \tau_3)(\tau_2 - \tau_3)} \qquad (21)$$

Differentiating eq 21 results in exit age distribution, i.e.

$$E(t) = \frac{\tau_1 e^{-t/\tau_1}}{(\tau_3 - \tau_1)(\tau_2 - \tau_1)} + \frac{\tau_2 e^{-t/\tau_2}}{(\tau_1 - \tau_2)(\tau_3 - \tau_2)} + \frac{\tau_3 e^{-t/\tau_3}}{(\tau_1 - \tau_3)(\tau_2 - \tau_3)} \qquad (22)$$

Case II: In this case, the three tanks are assumed to be equal in volume, i.e., $V_1 = V_2 = V_3$. Solving eqs 15 to 17 for the pulse input results in the following equation[17]

$$F(t) = \frac{t^2 e^{-t/\tau}}{2\tau^2} \qquad (23)$$

Equations 15−17 are solved for the exit age distribution for pulse input

$$E(t) = \frac{t^2 e^{-t/\tau}}{2\tau^3} \qquad (24)$$

While eqs 15−17 are solved for the step tracer input results, the following expression for $F(t)$ is seen

$$F(t) = 1 - \frac{t^2 e^{-t/\tau}}{2\tau^2} - e^{-t/\tau}\left(1 + \frac{t}{\tau}\right) \qquad (25)$$

Equation 24 is used for the $E(t)$ for the step input since the volumes are equal.

Case III: In this case, it is assumed that tanks 1 and 3 are equal in volume and the volume of tank 2 is higher than the others. Accordingly, eqs 15−17 are solved for pulse input, i.e.

$$F(t) = \frac{1}{(\tau_1 - \tau_2)}\left(te^{-t/\tau_1} + \frac{\tau_1\tau_2}{(\tau_1 - \tau_2)}(e^{-t/\tau_2} - e^{-t/\tau_1})\right) \qquad (26)$$

$E(t)$ can be obtained by differentiating eq 26, i.e.

$$E(t) = \frac{1}{\tau_1(\tau_1 - \tau_2)}\left(te^{-t/\tau_1} + \frac{\tau_1\tau_2}{(\tau_1 - \tau_2)}(e^{-t/\tau_2} - e^{-t/\tau_1})\right) \qquad (27)$$

Similarly eqs 15−17 are solved for the step input as

$$F(t) = 1 + \frac{\tau_1(2\tau_2 - \tau_1)e^{-t/\tau_1}}{(\tau_2 - \tau_1)^2} + \frac{te^{-t/\tau_1}}{(\tau_2 - \tau_1)} - \frac{{\tau_2}^2 e^{-t/\tau_2}}{(\tau_2 - \tau_1)^2} \qquad (28)$$

Differentiating eq 28 with respect to time results in the following expression for $E(t)$;

$$E(t) = \frac{(\tau_1 - 2\tau_2)e^{-t/\tau_1}}{(\tau_2 - \tau_1)^2} + \frac{e^{-t/\tau_1}}{(\tau_2 - \tau_1)}\left(1 - \left(\frac{t}{\tau_1}\right)\right) + \frac{\tau_2 e^{-t/\tau_2}}{(\tau_2 - \tau_1)^2} \qquad (29)$$

The model in eqs 19−29 gives the residence time distribution analysis of CSTER for different geometries. These equations are solved numerically and examined for critical operating conditions.

Experimental Section

The experimental setup given in Figure 2 consists of a glass beaker of 300 mL capacity with PVC lid having provision for

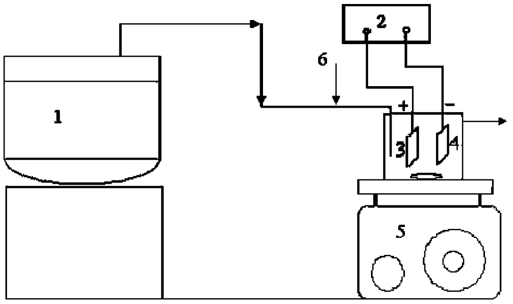

Figure 2. Schematic of continuous stirred tank electrochemical reactor experimental setup: (1) overhead tank; (2) dc power supply; (3) anode; (4) cathode; (5) magnetic stirrer; (6) tracer injection point.

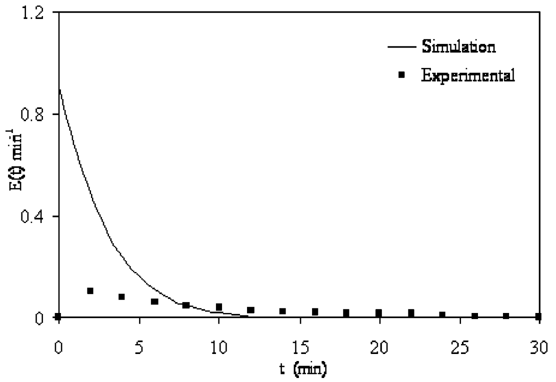

Figure 3. Comparison of model simulation of exit age distribution with experimental observation for the pulse input. $Q = 35$ mL min^{-1}; volume ratio = 1:3:2.

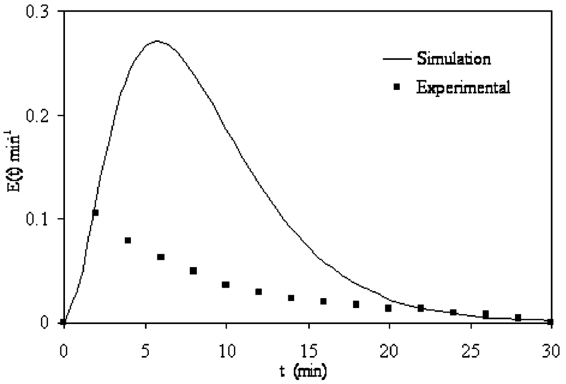

Figure 4. Comparison of model simulation of exit age distribution with experimental observation for the pulse input. $Q = 35$ mL min^{-1}; volume ratio = 1:1:1.

an anode and a cathode. RuO_2/Ti and a stainless steel sheet of 6.5×5 cm^2 were used as anode and cathode, respectively. The uniform electrolyte concentration inside the reactor has been maintained with the help of magnetic stirrer. Experiments were conducted on electrooxidation of dye effluent and residence time distribution to find the nonideality of the system without an electrochemical reaction.

For electrooxidation, synthetic effluent of Acid Red 88 dye has been prepared at various initial concentrations. The electrolysis was carried out under galvanostatic conditions using a dc-regulated power source (HIL model 3161). The effluent flow rate has been adjusted by adjusting throat valve and the samples were collected for analysis of color removal at steady state. For residence time distribution studies, the reactor was operated with water as electrolyte. The tracer of 10 mL of 1000 ppm Acid Red 88 dye solution was injected at steady state and sampled periodically at the outlet of the reactor and analyzed using a colorimeter.

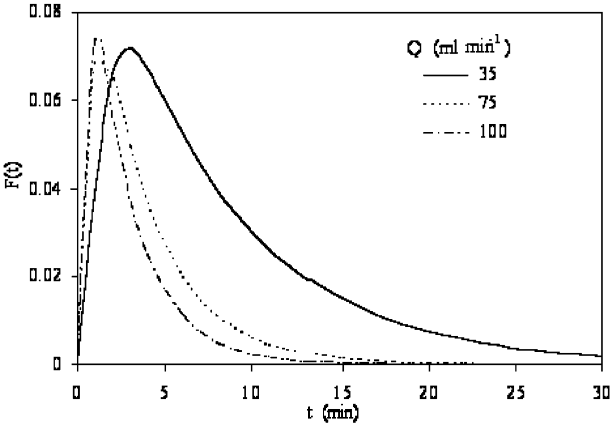

Figure 5. Simulated $F(t)$ distribution in a CSTER for a pulse input at different flow rates. Volume ratio = 1:10:1.

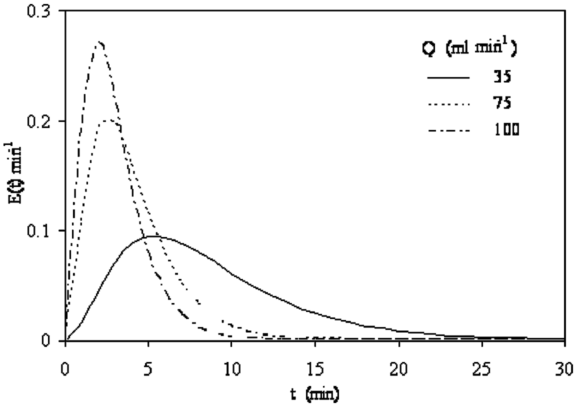

Figure 6. Simulated $E(t)$ distribution in a CSTER for a pulse input at different flow rates. Volume ratio = 1:2:1.

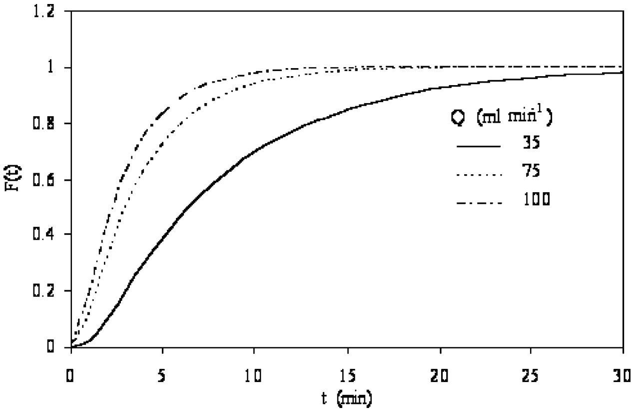

Figure 7. Simulated $F(t)$ distribution in a CSTER for a step input at different flow rates. Volume ratio = 1:10:1.

Results and Discussion

The electrolyte flow behavior in a continuous stirred tank electrochemical reactor has been simulated for both pulse and step tracer input using the model equations developed in the previous section. The exit age distribution $E(t)$ can be calculated from the tracer output using the following equation[18]

$$E(t) = \frac{c(t)}{\int_0^{\infty} c(t)\,\mathrm{d}t} \tag{30}$$

where $c(t)$ represent the exit tracer concentration at time “t” .

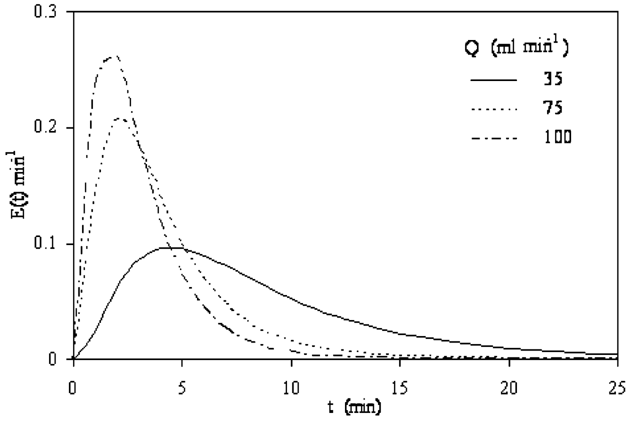

Figure 8. Simulated $E(t)$ distribution in a CSTER for a step input at different flow rates. Volume ratio = 1:4:1.

The mean residence time, variance, and the number of tanks in series can be calculated using the following equation.

The mean residence time distribution, for CSTER can be given as

$$\tau = \int_0^\infty tE(t)\,dt \tag{31}$$

The variance for CSTER can be written as

$$\sigma^2 = \int_0^\infty (t - \tau)^2 E(t)\,dt \tag{32}$$

The number of tanks, N, can be given as

$$N = \frac{\tau^2}{\sigma^2} \tag{33}$$

The number of tanks in the "tanks in series model" can be calculated using eq 33. The experimental observations and theoretical analysis of all three cases are discussed below.

Case I. The model equations developed in the earlier section [i.e., equations 19 to 22] have been solved for $E(t)$ and $F(t)$ distribution under various flow conditions. Figure 3 shows the simulated exit age distribution along with experimental observation for the pulse input. It can be ascertained from Figure 3 that the simulated exit age distribution shows wide deviation from experimental observations. Similar observation has been recorded for all the flow conditions. This may be the fact that the assumption considered in case I may not be realistic in electrochemical system.

Case II. Equations 23−25 have been solved for $E(t)$ and $F(t)$ distribution for both pulse and step inputs. Figure 4 compares the simulated exit age distribution along with experimental observation for pulse input. It can be noticed from Figure 4 that the simulated exit age distribution shows a much greater difference with the experimental observation. The deviation can be explained by the fact that the assumption of equal division of electrochemical reactor into three tanks in series does not reflect a realistic representation of the system. Similar observations have been noticed for all the other flow conditions also.

Case III. Equations 26−29 have been solved for $F(t)$ and $E(t)$ distribution for both step and pulse inputs for various electrolyte flow rates at different volume ratio of the tanks. Further the tanks in CSTER (tanks 1, 2, and 3) are assumed to have three volume ratios, i.e., 1:2:1; 1:4:1 and 1:10:1. Accordingly, the simulations have been carried out for the three volume ratios under various electrolyte flow rates, and the simulated results are presented in Figures 5 and 6. Figure 5 shows the simulated $F(t)$ for pulse input for the volume ratio 1:10:1. It can be ascertained from the figure that the $F(t)$ decreases with increase in the electrolyte flow rate. This is due to the fact that the volume by volumetric flow rate of the electrolyte decreases with increase in electrolyte flow rate resulting reduction in mean residence time distribution. It can also be observed from Figure 5 that the average residence time is decreases with increase in electrolyte flow rate. Similar observation has been recorded for the other volume ratios.

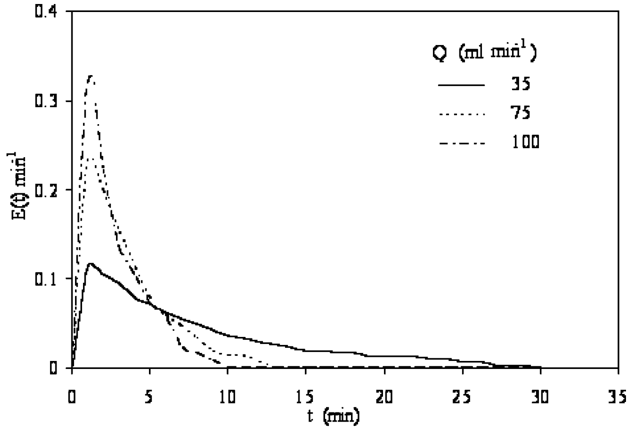

Figure 9. Experimental observation of $E(t)$ distribution in a CSTER for pulse input.

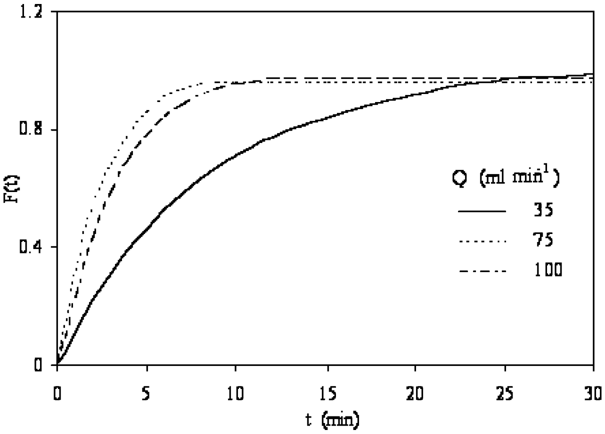

Figure 10. Experimental observation of $F(t)$ distribution in a CSTER for step input.

Figure 6 shows the simulated exit age distribution function $E(t)$ for pulse input at a 1:2:1 volume ratio. It can be ascertained from the figure that the $E(t)$ decreases with increase in electrolyte flow rate. This can be explained that the volume by volumetric flow rate decreases with increase in electrolyte flow rate resulting reduction in mean residence time distribution. Further it can be observed from Figure 6 that the average residence time decreases with an increase in electrolyte flow rate. On the other hand, Figures 7 and 8 show the simulation of $F(t)$ at 1:10:1 volume ratio and $E(t)$ simulation at 1:4:1 volume ratio, respectively. A similar observation has been observed for $F(t)$ and $E(t)$ distributions for the step input.

The experimental, analyzed for $E(t)$ and $F(t)$ distributions for different flow rates are given in Figures 9 and 10. It can be observed that the distributions of $E(t)$ and $F(t)$ decrease with an increase in flow rate of the electrolyte. Figure 11 shows the comparison of experimental observation with simulation for different volume ratios. It can be observed from the figure that the simulated results obtained for a volume ratio of 1:10:1

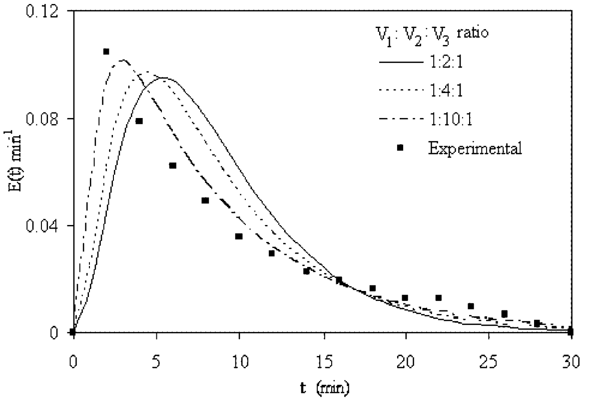

Figure 11. Comparison of simulated $E(t)$ distribution with experimental observation in a CSTER for pulse input. $Q = 35$ mL min^{-1}.

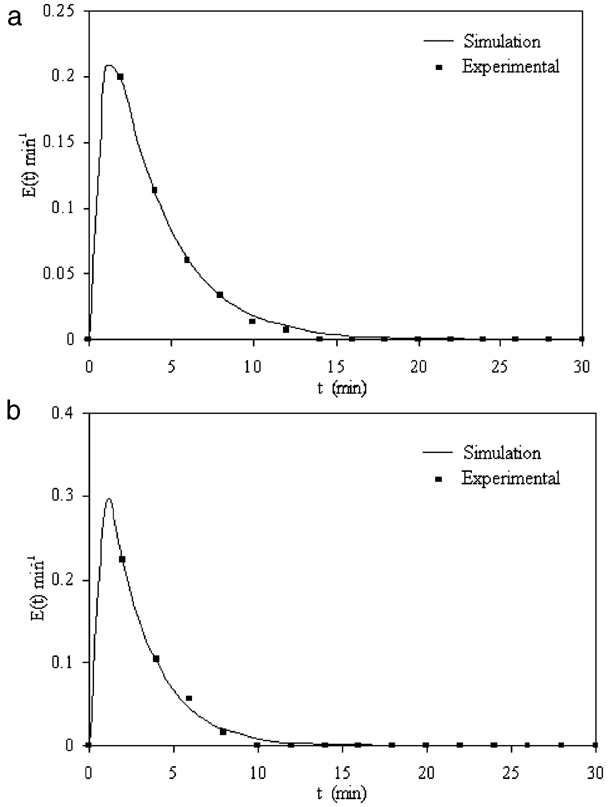

Figure 12. Comparison of model simulations of $E(t)$ distribution with the experimental observations: (a) $Q = 75$ mL min^{-1}; (b). $Q = 100$ mL min^{-1}.

matches satisfactorily with the experimental observation. While the other volume ratios (1:2:1 &1:4:1) give wide difference with the experiential observation. In fact the volume ratio of 1:10:1 refers to the point that tank 2 has a higher volume than the other two tanks, resulting in a maximum volume availability for the electrode process. This is a new observation recorded in the present investigation. The same trend has been recorded for all the electrolyte flow rates used in the present investigation.

Figures 12 and 13 show the comparison of simulated $E(t)$ and $F(t)$ with the experimental observation for pulse input and step input for the volume ratio of 1:10:1. It can be ascertained from the figures the simulated $E(t)$ and $F(t)$ distribution satisfactorily matches with the experimental observation. The effective volume of the tanks and for the different flow rates are given in Table 1. It can be observed from the table that the active volume (i.e., v_2) increased marginally with the flow rate of the electrolyte. The marginal increase in active volume occupied by the side compartment also was subjected to the process due to increased mixing with the electrolyte flow rates.

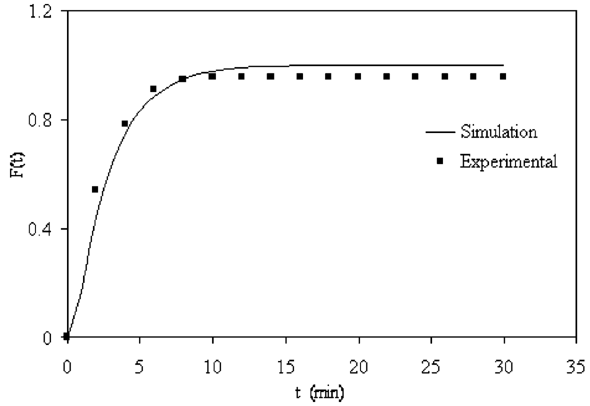

Figure 13. Comparison of model simulations of $F(t)$ distribution with the experimental observations, $Q = 100$ mL min^{-1}.

Table 1. Variation of Reactor Active Volumes (V_1, V_2) with Electrolyte Flow Rate

Q (mL min^{-1}	V_1 (cm^3)	V_2 (cm^3)
35	25	250
75	23	254
100	21	258

Table 2. Comparison of Theoretical and Experimental Decolorization Efficiency in the CSTER for Current Density 10 mA cm^{-2}, Initial Effluent Concentration 100 mg L^{-1}, and Supporting Electrolyte Concentration 1000 mg L^{-1}.

S. no.	Q (mL min^{-1})	τ (min)	no. of tanks	% decolorization	
				theor	exptl
1	35	7.08	1.18	67.42	60.50
2	75	3.09	1.49	54.79	52.23
3	100	2.40	1.59	49.98	42.67

Decolorization Efficiency. The theoretical analysis further extended to calculate the color removal efficiency using eq 14. Table 1 gives the number of tanks connected in series and the mean residence time. The mass transfer coefficient can be calculated using the following equation:

$$Ln\left(\frac{C}{C_i}\right) = \frac{-k_m S}{V} t \qquad (34)$$

k_m is the mass transfer coefficient. The experimental percentage color removal can be calculated using the following relation:

$$\%\ \text{decolorization} = \frac{C_i - C}{C_i} \times 100 \qquad (35)$$

The theoretical decolorization efficiency is good agreement with the experimental decolorization efficiency and the values are also given in Table 2.

Conclusion

Experiments were carried out in a continuous stirrer electrochemical reactor to study the residence time distribution and color removal covering a wide range in operating conditions. The electrolyte flow behavior has been experimented upon using both pulse and step input techniques, and the exit age distribution curves obtained under various operating conditions are critically analyzed. A *tanks in series model* has been developed to describe the electrolyte flow behavior inside the reactor and the model has been simulated under various conditions. It has been observed that the simulation for the volume ratio of 1:10:1 match well with experimental observations. Further it has been observed that the flow rate increases the reactor active volume. The model simulation has been used to determine the color removal efficiency and observed that the color removal efficiency predicted using present model matches satisfactorily with experimental observations.

Appendix

Analytical Solution for the Model Proposed. Case I. All three tanks are of different volumes. So the residence time of the each tank is different and is represented by τ_1, τ_2, and τ_3 for tank 1, tank 2, and tank 3, respectively.

For the first tank, the tracer material balance can be written as

$$\tau_1 \frac{dC_1}{dt} = C_0 - C_1 \tag{A1}$$

For tank 2, the material balance can be written as

$$\tau_2 \frac{dC_2}{dt} = C_1 - C_2 \tag{A2}$$

Similarly, for tank 3, the balance becomes

$$\tau_3 \frac{dC_3}{dt} = C_2 - C_3 \tag{A3}$$

Equations A1−A3 are solved for pulse input of tracer, and then eq A1 becomes

$$\frac{C_1}{C_0} = e^{-t/\tau_1} \tag{A4}$$

The A4 value is substituted into eq A2, and the solution can be written as

$$\frac{C_2}{C_0} = \frac{1}{\tau_2\left(\frac{1}{\tau_2} - \frac{1}{\tau_1}\right)}\left(e^{-t/\tau_1} - e^{-t/\tau_2}\right) \tag{A5}$$

The eq A5 value is substituted into eq A3 and the solution becomes

$$\frac{C_3}{C_0} = F(t) = \tau_1\left(\frac{\tau_1 e^{-t/\tau_1}}{(\tau_1 - \tau_2)(\tau_1 - \tau_3)} + \frac{\tau_2 e^{-t/\tau_2}}{(\tau_2 - \tau_1)(\tau_2 - \tau_3)} + \frac{\tau_3 e^{-t/\tau_3}}{(\tau_3 - \tau_2)(\tau_3 - \tau_1)}\right) \tag{A6}$$

Equation A6 is differentiated, and $E(t)$ becomes

$$E(t) = \tau_1\left(\frac{e^{-t/\tau_1}}{(\tau_1 - \tau_2)(\tau_3 - \tau_1)} + \frac{e^{-t/\tau_2}}{(\tau_1 - \tau_2)(\tau_2 - \tau_3)} + \frac{e^{-t/\tau_3}}{(\tau_2 - \tau_3)(\tau_3 - \tau_1)}\right) \tag{A7}$$

Then eqs A1−A3 are solved for step input of tracer. Equation A1 becomes

$$\frac{C_1}{C_0} = 1 - e^{-t/\tau_1} \tag{A8}$$

The eq A8 value is substituted into eq A2, and the equation solution can written as

$$\frac{C_2}{C_0} = 1 - \frac{\tau_1 e^{-t/\tau_1}}{\tau_1 - \tau_2} + \frac{\tau_2 e^{-t/\tau_2}}{\tau_1 - \tau_2} \tag{A9}$$

The eq A9 value is substituted into eq A3, and C_3 can be written as

$$\frac{C_3}{C_0} = F(t) = \left(1 - \frac{{\tau_1}^2 e^{-t/\tau_1}}{(\tau_3 - \tau_1)(\tau_2 - \tau_1)} - \frac{{\tau_2}^2 e^{-t/\tau_2}}{(\tau_1 - \tau_2)(\tau_3 - \tau_2)} - \frac{{\tau_3}^2 e^{-t/\tau_3}}{(\tau_1 - \tau_3)(\tau_2 - \tau_3)}\right) \tag{A10}$$

The A10 equation is differentiated and the $E(t)$ become

$$E(t) = \left(\frac{\tau_1 e^{-t/\tau_1}}{(\tau_3 - \tau_1)(\tau_2 - \tau_1)} + \frac{\tau_2 e^{-t/\tau_2}}{(\tau_1 - \tau_2)(\tau_3 - \tau_2)} + \frac{\tau_3 e^{-t/\tau_3}}{(\tau_1 - \tau_3)(\tau_2 - \tau_3)}\right) \tag{A11}$$

Case II. All the three tanks are of equal volume, and the residence time (τ) of each tank is same in all of the tanks.

The material balance of the tank 1 can be written as

$$\tau \frac{dC_1}{dt} = C_0 - C_1 \tag{A12}$$

Tank 2 can be written as

$$\tau \frac{dC_2}{dt} = C_1 - C_2 \tag{A13}$$

Similarly, for tank 3

$$\tau \frac{dC_3}{dt} = C_2 - C_3 \tag{A14}$$

Equations A12−A14 are solved for pulse input of tracer. Equation A12 can be written as

$$\frac{C_1}{C_0} = e^{-t/\tau} \tag{A15}$$

Substitute the C_1 into eq A13 and C_2/C_0 becomes

$$\frac{C_2}{C_0} = \frac{t e^{-t/\tau}}{\tau} \tag{A16}$$

Substitute the above value into eq A14 and C_3/C_0 can be written as

$$\frac{C_3}{C_0} = F(t) = \frac{t^2 e^{-t/\tau}}{2\tau^2} \tag{A17}$$

Differentiating the $F(t)$, $E(t)$ becomes

$$E(t) = \frac{t^2 e^{-t/\tau}}{2\tau^3} \tag{A18}$$

Equations A12−A14 are solved for step input of tracer, and C_1 can be written as

$$\frac{C_1}{C_0} = 1 - \mathrm{e}^{-t/\tau} \tag{A19}$$

Substitute the C_1 value into eq A13 to get the C_2 value

$$\frac{C_2}{C_0} = 1 - \frac{t\mathrm{e}^{-t/\tau}}{\tau} - \mathrm{e}^{-t/\tau} \tag{A20}$$

Substitute this value into eq A14 to get the C_3

$$\frac{C_3}{C_0} = F(t) = 1 - \frac{t^2\mathrm{e}^{-t/\tau}}{2\tau^2} - \mathrm{e}^{-t/\tau}\left(1 + \frac{t}{\tau}\right) \tag{A21}$$

Equation A21 is differentiated, and $E(t)$ becomes

$$E(t) = \frac{t^2\mathrm{e}^{-t/\tau}}{2\tau^3} \tag{A22}$$

Case III. In this case tank 1 and tank 2 are of equal volumes and the tank 3 volume is greater than these two. τ_1 and τ_3 are residence times of tanks 1 and 3 respectively, and τ_2 is the residence time of tank 2.

For tank 1, the tracer material balance can be written as

$$\tau_1 \frac{\mathrm{d}C_1}{\mathrm{d}t} = C_0 - C_1 \tag{A23}$$

For tank 2, the balance becomes

$$\tau_2 \frac{\mathrm{d}C_2}{\mathrm{d}t} = C_1 - C_2 \tag{A24}$$

Similarly for tank 3

$$\tau_1 \frac{\mathrm{d}C_3}{\mathrm{d}t} = C_2 - C_3 \tag{A25}$$

Equations A23−25 can be solved for pulse input of tracer. C_1 can be written as

$$\frac{C_1}{C_0} = \mathrm{e}^{-t/\tau_1} \tag{A26}$$

The above value is substituted into eq 24, and C_2 becomes

$$\frac{C_2}{C_0} = \frac{1}{\tau_2\left(\frac{1}{\tau_2} - \frac{1}{\tau_1}\right)}(\mathrm{e}^{-t/\tau_1} - \mathrm{e}^{-t/\tau_2}) \tag{A27}$$

The C_2 value is substituted into eq A25, and C_3 becomes

$$\frac{C_3}{C_0} = F(t) = \frac{1}{\tau_1 - \tau_2}\left(t\mathrm{e}^{-t/\tau_1} + \frac{\tau_1\tau_2\mathrm{e}^{-t/\tau_2}}{(\tau_1 - \tau_2)}(\mathrm{e}^{-t/\tau_2} - \mathrm{e}^{-t/\tau_1})\right) \tag{A28}$$

Differentiating eq A28, the $E(t)$ equation becomes

$$E(t) = \frac{1}{\tau_1(\tau_1 - \tau_2)}\left(t\mathrm{e}^{-t/\tau_1} + \frac{\tau_1\tau_2}{(\tau_1 - \tau_2)}(\mathrm{e}^{-t/\tau_2} - \mathrm{e}^{-t/\tau_1})\right) \tag{A29}$$

Equations A23−A25 can be solved for step input of tracer

$$\frac{C_1}{C_0} = 1 - \mathrm{e}^{-t/\tau_1} \tag{A30}$$

C_1 is substituted into eq A24, and C_2 is written as

$$\frac{C_2}{C_0} = 1 - \frac{\tau_1\mathrm{e}^{-t/\tau_1}}{\tau_1 - \tau_2} + \frac{\tau_2\mathrm{e}^{-t/\tau_2}}{\tau_1 - \tau_2} \tag{A31}$$

C_2 is substituted into eq A25, and C_3 is written as

$$\frac{C_3}{C_0} = F(t) = 1 + \frac{\tau_1(2\tau_2 - \tau_1)\mathrm{e}^{-t/\tau_1}}{(\tau_2 - \tau_1)^2} + \frac{t\mathrm{e}^{-t/\tau_1}}{(\tau_2 - \tau_1)} - \frac{{\tau_2}^2\mathrm{e}^{-t/\tau_2}}{(\tau_2 - \tau_1)^2} \tag{A32}$$

Differentiating eq A32, the $E(t)$ equation becomes

$$E(t) = \frac{(\tau_1 - 2\tau_2)\mathrm{e}^{-t/\tau_1}}{(\tau_2 - \tau_1)^2} + \frac{\mathrm{e}^{-t/\tau_1}}{(\tau_2 - \tau_1)}\left(1 - \left(\frac{t}{\tau_1}\right)\right) + \frac{\tau_2\mathrm{e}^{-t/\tau_2}}{(\tau_2 - \tau_1)^2} \tag{A33}$$

Nomenclature

υ = volumetric flow rate
$C_{\mathrm{A}i}$ = inlet concentration
C_{A} = outlet concentration
$C_{\mathrm{A}}^{\mathrm{S}}$ and $C_{\mathrm{B}}^{\mathrm{S}}$ = surface concentration of reactant and product at the electrode
I = applied current
i = current density
S = surface area of the electrode
n = number of electrons
N = number of tanks in series
F = Faraday law constant
σ =surface area per unit volume
τ = residence time
σ^2 = variance
k_{L1} and k_{L2} = mass transfer coefficients
D_1 and D_2 = Damkohler numbers

Literature Cited

(1) Razo-Flores, E.; Luijten, M.; Donlon, B.; Lettinga, G.; Field, J. Biodegradation of selected azo dyes under methanogenic conditions. *Water Sci. Technol.* **1997**, *36*, 65.

(2) Lin, S. H.; Peng, F. C. Treatment of textile wastewater by electrochemical methods. *Water Res.* **1994**, *2*, 277.

(3) Walsh, F. C. Electro chemical technology for environmental treatment and clean energy conversion. *Pure Appl. Chem.* **2001**, *73*, 1819.

(4) Mohan, N.; Balasubramanian, N.; Subramanian, V. Electrochemical treatment of simulated textile effluent. *Chem. Eng. Technol.* **2001**, *24*, 749.

(5) Mohan, N.; Balasubramanian, N. In situ electro catalytic oxidation of acid violet 12 dye effluent. *J. Hazard. Mater.* **2006**, *B136*, 239.

(6) Mohan, N.; Balasubramanian, N.; Ahmed Basha, C. Electro chemical oxidation of textile wastewater and its reuse. *J. Hazard. Mater.* **2007**, *147*, 644.

(7) Bengoa, C.; Montillet, A.; Legentilhomme, A.; Legrand. J. Flow visualization and modelling of a filter-press type electrochemical reactor. *J. Appl. Electrochem.* **1997**, *27*, 1313.

(8) Szpyrkowicz, L.; Radaelli, M. Scale-up of an electrochemical reactor for treatment of industrial wastewater with an electrochemically generated redox mediator. *J. Appl. Electrochem.* **2006**, *36*, 1151.

(9) Trinidad, P.; Walsh, F. C. Hydrodynamic Behavior of the FM01-LC reactor. *Electrochim. Acta* **1996**, *41*, 493.

(10) Trinidad, P.; Walsh, F. Conversion expressions for electrochemical reactors which operate under mass transport controlled reaction conditions, Part I: Batch Reactor, PFR and CSTR. *Int. J. Eng. Ed.* **1998**, *14*, 431.

(11) Carpenter, N. G.; Roberts, E. P. L. Mass transport and residence time characteristics of an oscillatory flow electrochemical reactor. *Chem. Eng. Res. Des.* **2007**, *77*, 212.

(12) Gonza lez-Garcya, J.; Montiel, V.; Aldaz, A.; Conesa, J. A.; Perez, J. R.; Codina, G. Hydrodynamic behavior of a filter-press electro chemical reactor with carbon felt as a three-dimensional electrode. *Ind. Eng. Chem. Res.* **1998**, *37*, 4501.

(13) Polcaro, A. M.; Vacca, A.; Mascia, M.; Palmas, S.; Pompei, R.; Laconi, S. Characterization of a stirred tank electrochemical cell for water disinfection processes *Electrochim. Acta* **2007**, *52*, 2595.

(14) Scott. K. The continuous stirred tank electrochemical reactor. An overview of dynamic and steady state analysis for design and modeling. *J. Appl. Electrochem.* **1991**, *21*, 945.

(15) Vijayasekaran, B.; Ahmed Basha, C. Modeling in electrochemical engineering−a critical review. *Trans. SAEST* **2005**, *40*, 1.

(16) Scott, K. *Electrochemical Reaction Engineering*; Academic Press: London, 1991.

(17) Scott Fogler, H. *Elements of Chemical Reaction Engineering*, 2nd ed.; Prentice Hall International: Englewood Cliffs, NJ, 1992.

(18) Levenspiel, O. *Chemical Reaction Engineering*; John Wiley & Sons: New York, 1999.

Received for review October 21, 2007
Revised manuscript received January 31, 2008
Accepted February 12, 2008

IE071426Q